Vol. 52: 159–174, 2012
doi: 10.3354/cr01077

CLIMATE RESEARCH
Clim Res

Published March 22

Contribution to CR Special 29 'The regional climate model RegCM4'

Effects of coastal topography on climate: high-resolution simulation with a regional climate model

Barış Önol*

Istanbul Technical University, Aeronautics & Astronautics Faculty, Meteorological Engineering, Maslak, 34469 Istanbul, Turkey

ABSTRACT: High-resolution regional climate simulations driven by NCEP-reanalysis for the eastern Mediterranean (EM) region covering 48 yr (1961–2008) are used to examine the coastal effects over the EM region. The present study uses the ICTP-RegCM3 to downscale to a 10 km resolution over the EM with a 50 km driving nest. The high-resolution simulation captures strong temperature gradients as a result of resolving the steep topography over the eastern Black Sea and Mediterranean coasts of Turkey, as well as the Ionian coast of Greece. In terms of the validation based on the coastal meteorological stations, the annual temperature bias in the high-resolution simulation is <0.7°C for the Black Sea and Mediterranean regions over Turkey and the same bias is 1°C in the 50 km simulation. Moreover, the model is able to capture the observed warming trend in summer temperatures during the last 5 decades. In terms of the precipitation simulation, the error in the 10 km simulation (17%) over the Black Sea region is much lower than that in the 50 km simulation (42%) when considering coastal meteorological stations. In addition, existence of many small islands over the EM domain is another unresolved challenge for climate simulations. The small islands tend to be overwhelmed by the influence of sea-surface temperature, and local climate effects related to topography are suppressed in 10 km temperature simulations. However, the precipitation error in the 10 and 50 km simulations based on the island stations (Crete, Rhodes and Cyprus) over the EM domain are 12 and 24%, respectively. In terms of the cross-section analysis comparing model elevation to simulated precipitation, the implementation of high-resolution simulation illustrates the importance of modeling the complex terrain over the eastern Black Sea and Mediterranean coasts of Turkey, as the precipitation error was reduced to 7 and 18%, respectively.

KEY WORDS: Coastal effect on climate · Regional climate modeling · Eastern Mediterranean

1. INTRODUCTION

The Mediterranean region is emerging as the primary responsive region to human-induced climate change (Giorgi 2006). More precisely, the eastern Mediterranean (EM) countries are more vulnerable to climate change than other Mediterranean countries because of their accelerated population growth accompanied by projected poverty growth (Diffenbaugh et al. 2005). Most of the population in this region lives in coastal areas. Therefore, it is very important to carry out a sensitivity analysis on the horizontal resolution of the model for coastal regions, in order to understand the local forcing impact on the regional climate.

The horizontal resolution used for current regional climate simulations over most of the region is generally around 20 to 50 km. However, the complexity of topographical features may play a crucial role in determining the model resolution needed. Therefore,

*Email: onolba@itu.edu.tr

any insufficiency in the horizontal resolution may produce serious deficiencies in climate simulations over some specific regions. Since the land surface in the EM region is very complex, including the steep terrain of the Black Sea coast and the complex land–sea interface along the coasts of Greece and western Turkey, the present study tests the impact of horizontal model resolution for surface temperature and precipitation. Moreover, the existence of many small islands in the Aegean Sea is another unresolved challenge for climate simulations; higher resolutions will help to provide a more accurate representation of the climate for these small islands.

Many modeling studies have been conducted by using regional climate models over the EM domain (Evans et al. 2004, Krichak et al. 2007, Gao & Giorgi 2008, Önol & Semazzi 2009, Zanis et al. 2009, Bozkurt & Sen 2011, Bozkurt et al. 2011). The finest model resolution used in these previous studies was 20 km and demonstrated that limited area models have a strong positive precipitation bias for the wet seasons over mountain ranges, which are very steep along the coastline. Using a higher resolution regional climate simulation may provide a valuable contribution in resolving potential model errors, as higher resolutions help to more accurately define land-surface properties. Christensen et al. (1998) pointed out that a high-resolution (19 km) regional climate simulation performed better than an intermediate-resolution (57 km) simulation for surface variables (2 m temperature, precipitation and runoff) over the Scandinavian Peninsula, where many fine-scale topographical features such as narrow mountain ridges and complicated land-sea contrasts dominate the local climate. In the present study, a double nesting approach is used, whereby the output from the first domain run at 50 km resolution sets the boundary conditions for the higher resolution (10 km) domain. These simulations were run for several decades of continuous data (1961–2008).

A horizontal grid spacing of 10 km is the finest resolution used within the model ICTP-RegCM3 (Torma et al. 2011). In their study, the temporal and spatial variability of temperature and precipitation for the Carpathian Basin are discussed. The results indicate that the seasonal temperature biases for 10 km simulation are <1°C and the frequency of dry and wet spells is well reproduced by the model. They encouraged testing the use of higher resolution with RegCM3 for extra-tropical regions. The RegCM3 has also been used for applying mosaic-type parameterization of subgrid-scale topography in the alpine region, where the subgrid cell size is 3 km (Im et al. 2010). In addition, studies using different regional models have indicated the added precision of using higher horizontal resolution (Sotillo et al. 2005, Kanamitsu & Kanamaru 2007, Prömmel et al. 2010). In particular, Di Luca et al. (2011) recently discussed the added precision for simulated precipitation using 6 different regional climate models.

A recent project called the coordinated regional climate downscaling experiment (CORDEX) attempts to generate an ensemble of simulations in order to understand all the relevant uncertainty dimensions for the different domains of the world (Giorgi et al. 2009). The 50 km resolution domain in the present study covers the European-CORDEX domain and extends to mid-Asia and mid-Africa. Therefore, this study may supply useful information for CORDEX studies based on the European domain. Additionally, this is the first implementation of RegCM3 at a 10 km resolution for the EM domain and will provide useful information on the impact of horizontal resolution for future regional climate modeling studies of the EM region.

2. SIMULATION DESIGN AND DATA

In the present study, simulation of a 48 yr continuous period from 1961 to 2008 was carried out using the International Centre for Theoretical Physics regional climate model, Version 3 (ICTP-RegCM3) for 2 domains using a nest-down approach — a 50 km (mother) and 10 km (nested) domain (Fig. 1, upper panel). The mother domain simulation, covering Europe, North Africa and most of the Middle East, is driven by the NCEP/NCAR reanalysis (Kalnay et al. 1996). One year spin-up time was applied for simulation of the mother domain starting in January 1960. The EM domain was selected as the nested domain because of its complex topography, land-sea distribution and large contrasts in vegetation (Fig. 1, lower panel), which play a crucial role in modulating the atmospheric parameters over the entire domain. Both simulations have been validated by gridded and station observations.

2.1. ICTP-RegCM3

The ICTP-RegCM3 is a 3-dimensional hydrostatic atmospheric model using a sigm a-pressure-based vertical coordinate system. The radiation transfer package is based on the National Center for Atmospheric Research (NCAR) coupled climate model,

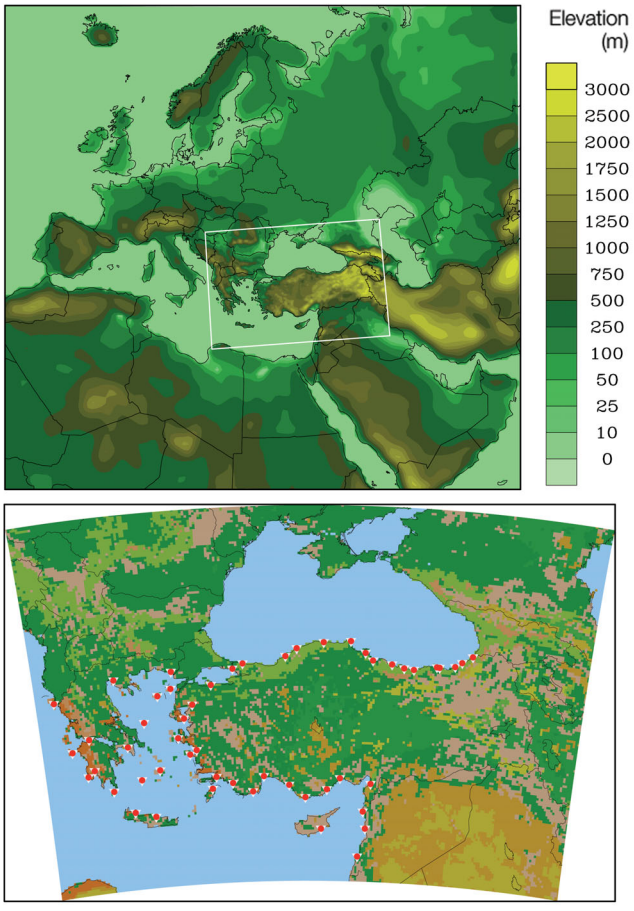

Fig. 1. Mother domain topography (50 km; upper panel) and nested domain land use (10 km; lower panel; colours represent vegetation types) of simulations. Red spots: locations of TSMS and GCN stations (see Table 1 for station details)

Version 3 (CCM3; Kiehl et al. 1996). The atmospheric component of the model is coupled with the land-surface model, called the Biosphere–Atmosphere transfer scheme (BATS; Dickinson et al. 1993), and the ocean-surface flux parameterization by Zeng et al. (1998). To simulate large-scale precipitation, the RegCM3 uses the SUBgrid explicit moisture scheme, called SUBEX (Pal et al. 2000). The Grell (1993) convective parameterization scheme with the Fritsch & Chappell (1980) closure formulation is used in the present study. Further details regarding the RegCM3 model are given in Pal et al. (2007). The vertical resolution of RegCM3 applied in our study has 18 sigma levels.

2.2. Observations

In terms of surface temperature and precipitation, different types of observational data were used for the validation of both the mother and nested simulations. Gridded observational datasets used in the present study were the Climatic Research Unit CL 2.0 (CRU-CL; New et al. 2002) and CRU-TS 3.0 (Mitchell & Jones 2005), the University of Delaware's UDEL, Version 2.01 (Willmott & Matsuura 1995), the Global Historical Climatology Network Version 2 and the Climate Anomaly Monitoring System analysis (GHCN-CAMS; Fan & van den Dool 2008) and the Global Precipitation Climatology Centre's GPCCv5, Version 5 (Rudolf et al. 1994) rain gauge precipitation dataset. Grid spacing of all these gridded datasets, except CRU-CL, is 0.5° × 0.5°. These datasets were used to evaluate the 50 km mother domain simulation. The CRU-CL dataset (10′, i.e. 10 minute grid-spacing), which consists of 30 yr (1961–1990) climatological means, was used to help with the validation of the 10 km domain simulation over the EM region. However, observational deficiencies over the mountainous regions of Turkey pose an important concern for observational versus model comparisons (Önol & Semazzi 2009). The difficulties related to the evaluation of RCM performance over complex terrain where it is constrained by sparse station networks have been noted by Giorgi et al. (2001). Therefore, a station versus grid-box method was applied to evaluate the 10 km domain. This method has been demonstrated to be effective for evaluating high-resolution regional climate model simulations (Kanamitsu & Kanamaru 2007, Prömmel et al. 2010). One of the main objectives of the present study was to determine how high-resolution simulations reproduce observed climate for the coastal region of the EM. To help with model evaluation, we have selected 52 stations located near the EM shoreline. The use of this additional data may facilitate more robust evaluation and eliminate orography-related problems.

The station-based observational datasets used in the present study were the Global Climate Normals (GCN) from the National Climatic Data Center and the Turkish State Meteorological Service (TSMS) dataset. A total of 30 meteorological stations for temperature and precipitation data were selected from the TSMS, and 22 meteorological stations from the GCN for Greece, Cyprus, Syria and Lebanon (Table 1), to help in illustrating the added precision of using higher horizontal resolution over complex terrain (Fig. 1, lower panel, red spots). The time periods 1961–1990 and 1971–2000 have been considered for GCN and TSMS stations, respectively. Since the station datasets cover 2 different time periods, analyses have been performed separately for each group of stations. These stations and corresponding model

Table 1. Information on meteorological stations (see red dots on Fig. 1, lower panel) used in the present study. TSMS: Turkish State Meteorological Service; GCN: Global Climate Normals

No.	Station	Latitude (°N)	Longitude (°E)	Period
TSMS				
Turkey				
17042	Hopa	41.40	41.43	1971–2000
17628	Pazar	41.18	40.88	
17040	Rize	41.03	40.52	1971–2004
17037	Trabzon	41.00	39.72	
17626	Akcaabat	41.02	39.58	1971–2000
17034	Giresun	40.92	38.40	1971–2004
17033	Ordu	40.98	37.90	1971–2000
17624	Unye	41.13	37.28	
17030	Samsun	41.28	36.30	
17622	Bafra	41.57	35.92	
17026	Sinop	42.02	35.17	1971–2004
17024	Inebolu	41.98	33.77	1971–2000
17602	Amasra	41.75	32.38	
17022	Zonguldak	41.45	31.80	
17610	Sile	41.17	29.60	
17062	Goztepe	40.97	29.08	
17114	Bandirma	40.35	27.97	
17110	Gokceada	40.20	25.90	
17696	Edremit	39.60	27.02	
17221	Cesme	38.32	26.30	
17232	Kusadasi	37.87	27.25	
17298	Marmaris	36.85	28.27	
17296	Fethiye	36.62	29.12	
17375	Finike	36.30	30.15	
17300	Antalya	36.88	30.70	1971–2004
17310	Alanya	36.55	32.50	
17320	Anamur	36.08	32.83	
17330	Silifke	36.38	33.93	
17340	Mersin	36.80	34.60	1971–2000
17370	Iskenderun	36.58	36.17	
GCN				
Greece				
16622	Thessaloniki	40.52	22.97	1961–1990
16627	Alexandroupolis	40.85	25.92	
16641	Kerkira	39.62	19.92	
16650	Limnos	39.92	25.23	
16667	Mitilini	39.07	26.60	
16684	Skiros	38.90	24.55	
16689	Patrai	38.25	21.73	
16714	Athens	37.97	23.72	
16719	Zakinthos	37.75	20.88	
16723	Samos	37.70	26.92	
16726	Kalamata	37.07	22.02	
16732	Naxos	37.10	25.38	
16734	Methoni	36.83	21.70	
16738	Milos	36.72	24.45	
16743	Kythira	36.28	23.02	
16746	Souda	35.48	24.12	
16749	Rhodes	36.40	28.08	
16754	Iraklion	35.33	25.18	
Cyprus				
17609	Larnaca	34.88	33.63	
Syria				
40022	Latakia	35.53	35.77	
40050	Tartous	34.88	35.88	
Lebanon				
40100	Beirut	33.82	35.48	

grid-points have been analyzed for both 10 and 50 km simulations by considering the annual means of temperature and precipitation and the corresponding biases. Moreover, variability of the simulated precipitation based on model grid-points was investigated for selected station locations. The lower panel in Fig. 1 illustrates all the station locations for TSMS and GCN.

3. RESULTS

The first approach is based on the analysis of the spatial distribution of surface temperature and precipitation to define model performance over the mother and nested simulation domains. In the second approach, station datasets are used to calculate biases for corresponding model grid-points. In addition, we use running averages and decadal anomalies for analysis of variability and trends.

3.1. Validation of the mother domain

The RegCM3 output of 50 km simulation has been analyzed with 4 different (CRU-TS, UDEL, GHCN-CAMS and GPCCv5) observational datasets. Evaluation of the 50 km simulation with these datasets, all of which have the same horizontal resolution (half a degree), provides a fundamental basis for defining uncertainty in model bias.

The 1971–2000 climatology is used for comparison of surface temperature for the 50 km simulation and 3 other datasets. The 50 km simulation reproduces annual mean temperatures realistically (Fig. 2). The simulated spatial distribution of temperature from the Scandinavian Peninsula to North Africa is consistent with observations. There is a warm bias of 3–5°C for the Alps and Caucasus Mountains, and this is mostly apparent when the simulations are compared with the CRU and UDEL datasets. The coarse resolution of 50 km is potentially responsible for the warm bias over mountainous regions. However, there is also a noticeable cold bias of 1–2°C in the 50 km simulation for the EM region, which is the area of interest in the present study for downscaling to 10 km.

Observations over the EM region have shown that heat waves are becoming more frequent (Kuglitsch et al. 2010) and will represent a significant threat to human welfare as the climate changes. Therefore, modeling extreme events, such as heat waves, is of significant importance for regional climate modeling. Additionally, a previous study has demonstrated that a regional climate model simulation can reproduce

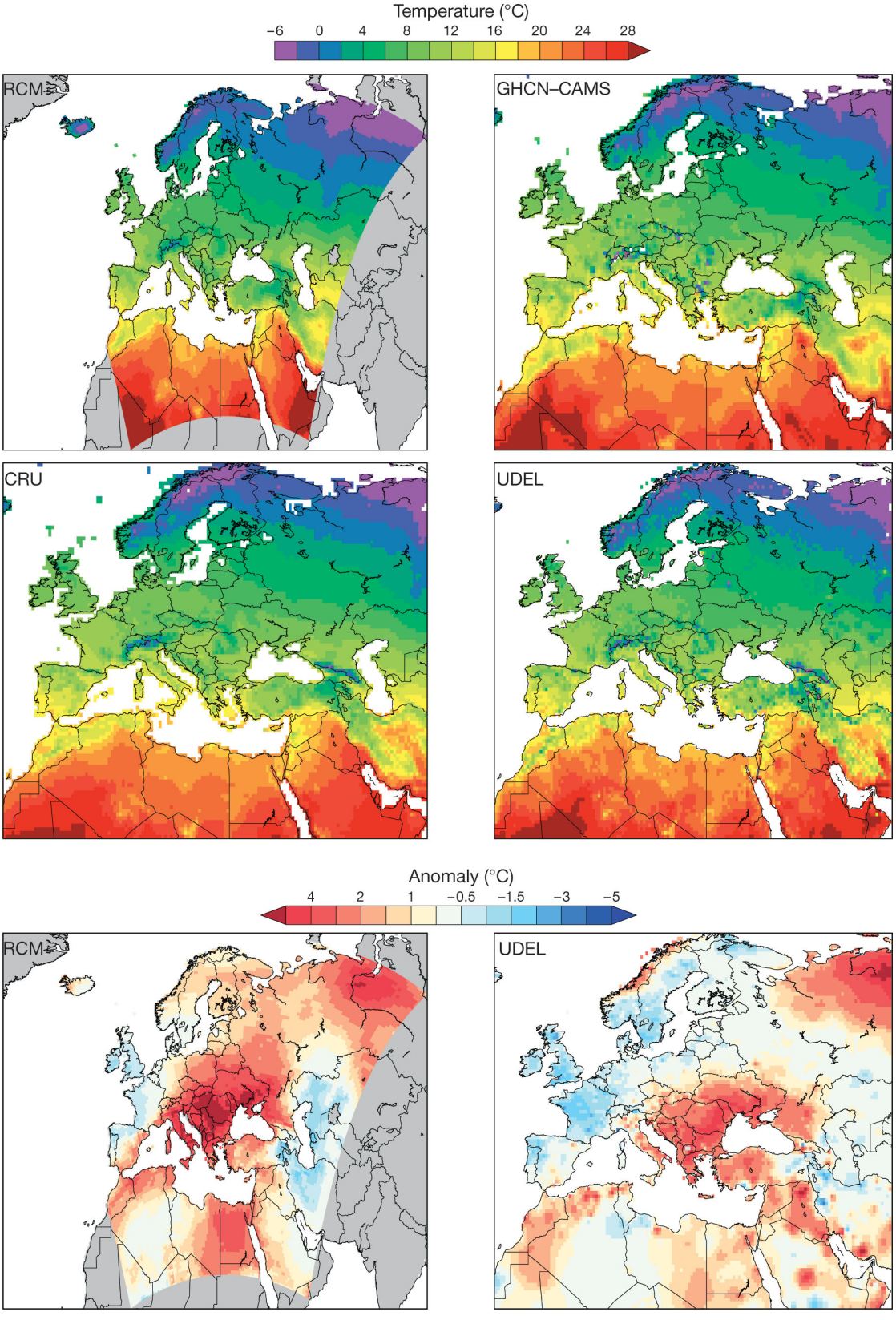

Fig. 2. Mean annual surface temperature (1971–2000) according to the RegCM3 mother simulation (RCM) and gridded observations (GHCN-CAMS, CRU and UDEL; see Section 2.2) (upper panels). Comparisons with the surface temperature anomaly (July 2007) between the RegCM mother domain simulation and gridded observation UDEL (lower panels)

extreme temperatures much more realistically than NCEP/NCAR reanalysis data (Sotillo et al. 2005). In the present study, we demonstrate the model's ability to simulate extreme temperature using snap-shot anomaly validation for the 2007 heat wave event that plagued southeastern Europe and the EM region. Fig. 2 (lower panels) is a plot of the July 2007 temperature anomaly relative to the mean for the 1971–2000 reference period. Since only the UDEL dataset covers the summer of 2007, RegCM3 simulation is evaluated using only this dataset. RegCM3 simulation captures the general pattern of the temperature anomaly. The simulated temperature anomaly covers most of Romania, Hungary and Serbia and exceeds 5°C, but the observations are nearly 2°C cooler than the 50 km simulation. However, the simulated magnitude of the anomaly is consistent with the observed anomaly over Greece and Turkey.

As for model validation of precipitation, we chose to compare the climatological means for the winter season because most precipitation occurs during this season over Europe and the EM domain. The mean values are for the 1971–2000 time period. The RegCM3 reproduces the general pattern of winter precipitation fairly well (Fig. 3). Latitudinal variation and orographic forcing are dominant factors influencing precipitation distribution. The 50 km simulation has a positive precipitation bias for most of the domain. This bias is around 20 to 30% over the lowlands and is more pronounced at higher elevations, especially over the Caucasus, Taurus and Zagros Mountains. However, the larger bias over mountainous regions may be a result of observational deficiency as has been discussed in a previous study (Önol & Semazzi 2009). Moreover, when comparing these regions with the Alps, we find a smaller bias in the 50 km simulation for the alpine region, which is likely a result of better observational coverage.

As for temperature, we selected an extreme event to better understand the model's ability to accurately simulate precipitation. In particular, we investigated the model's ability to simulate the precipitation associated with changes in the North Atlantic Oscillation (NAO). Negative (positive) phases of the NAO favor a wetter (drier) winter for the Mediterranean region (Hurrell 1995). One of the driest seasons (December–March, DJFM, 1988–1989), with the highest positive values of the NAO index, was selected to examine precipitation variability over the EM region. Fig. 3 illustrates that the RegCM3 realistically simulates the precipitation anomaly (reference period: 1971–2000) for this event when compared to precipitation in the GPCCv5 dataset.

3.2. Validation of the nested domain

Since the time period of the high-resolution (10′) observational dataset (CRU-CL) covers the years 1961–1990, spatial validations of the surface temperature and precipitation were performed for this period. Model and observation comparisons of spatial seasonal temperatures indicated that 10 km simulation has a 2°C cold bias over most of the model domain, except the mountainous region in the northeastern part of the domain, which has a warm winter bias (Fig. 4). The simulated temperature over the southeast of the domain is more consistent with CRU-CL observations and has a relatively smaller bias compared to the rest of the domain. We also note a robust cold bias pattern for the highlands in spring and summer, which may be a function of resolving the terrain with a higher resolution. The smallest temperature bias is found during autumn.

The simulated strong temperature gradients, as large as 20°C in a few places, are caused by steep topography in the eastern Black Sea region, along the Mediterranean coasts of Turkey and on the Ionian coast of Greece (Fig. 4). These strong temperature gradients, as a result of complex topography, are also seen in the observations but the gradient is not quite as strong as that modeled. Fig. 5 compares the 10 and 50 km temperature simulations for the Mediterranean coast of Turkey. The temperature gradient in January is clearer in the 10 km simulation than in the 50 km simulation compared to CRU-CL. To exemplify this, we compared mean temperatures over the Taurus Mountains; the observational and 10 km simulation temperatures are in the range of −7 to −9°C compared to −1 to −3°C for the 50 km simulation over the same region. Therefore, the higher resolution simulation adds value over this region.

In terms of precipitation, the high-resolution simulation enhances orographic forcing and can be seen as the precipitation following topography is more pronounced (Fig. 6). In the simulation precipitation is overestimated over mountain ranges, especially in the winter and spring, in comparison to the CRU-CL (Fig. 6). However, it is very difficult to quantify the precipitation bias, because the CRU-CL dataset does not capture the precipitation for all higher elevation areas and does not provide much additional information compared to the coarse-resolution dataset (0.5°, CRU-TS). This problem could be a result of the method applied in the interpolation of the CRU-CL data (New et al. 2002). In the study by New et al., the gamma distribution method was used to capture precipitation, but the authors applied elevation as a co-

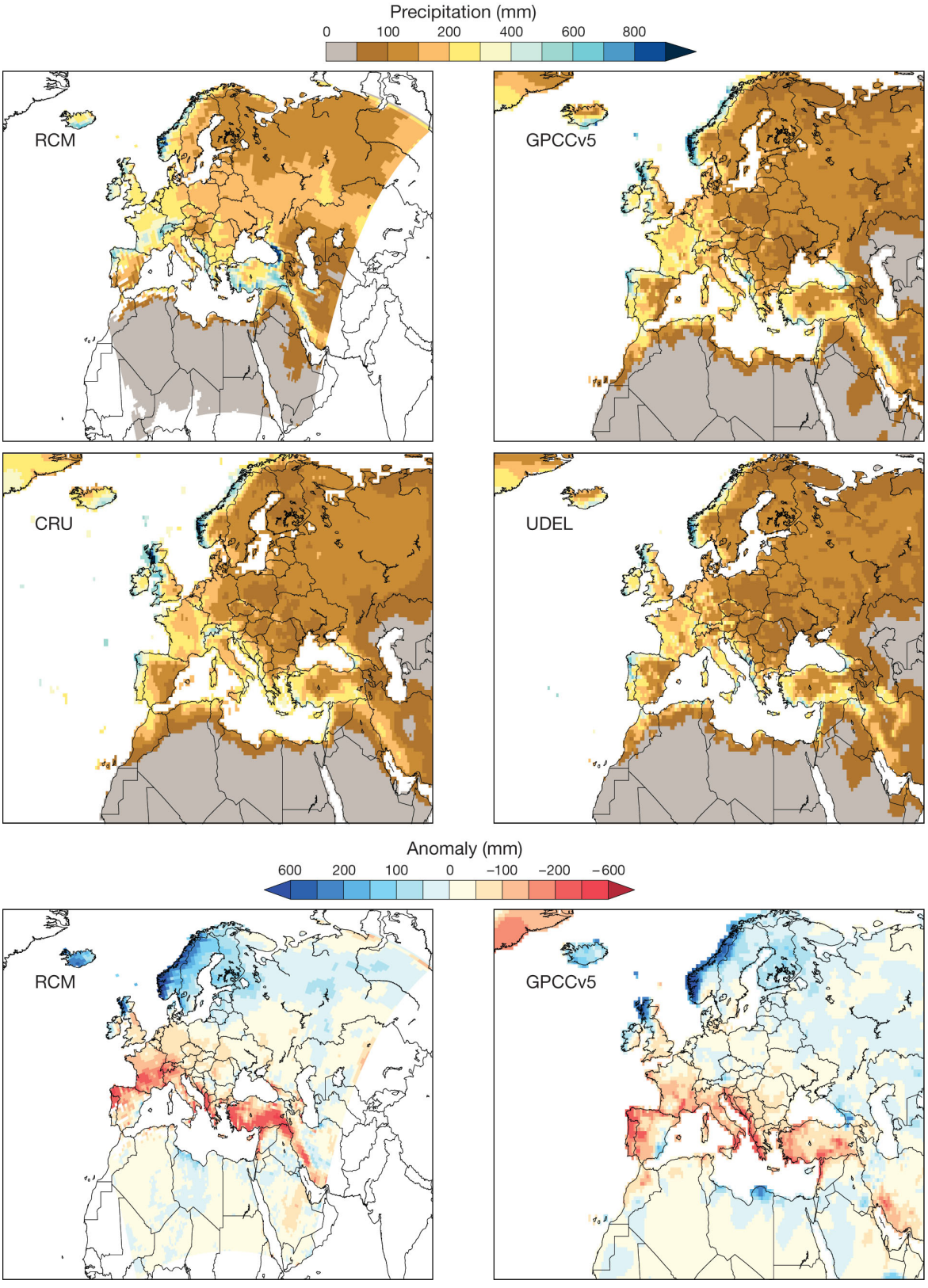

Fig. 3. Mean winter precipitation (1971–2000) according to the RegCM3 mother simulation (RCM) and gridded observations (GPCCv5, CRU and UDEL; see Section 2.2) (upper panels). Comparisons with the precipitation anomaly (December–March [DJFM] 1988/1989) between the RegCM mother domain simulation and gridded observation GPCCv5 (lower panels)

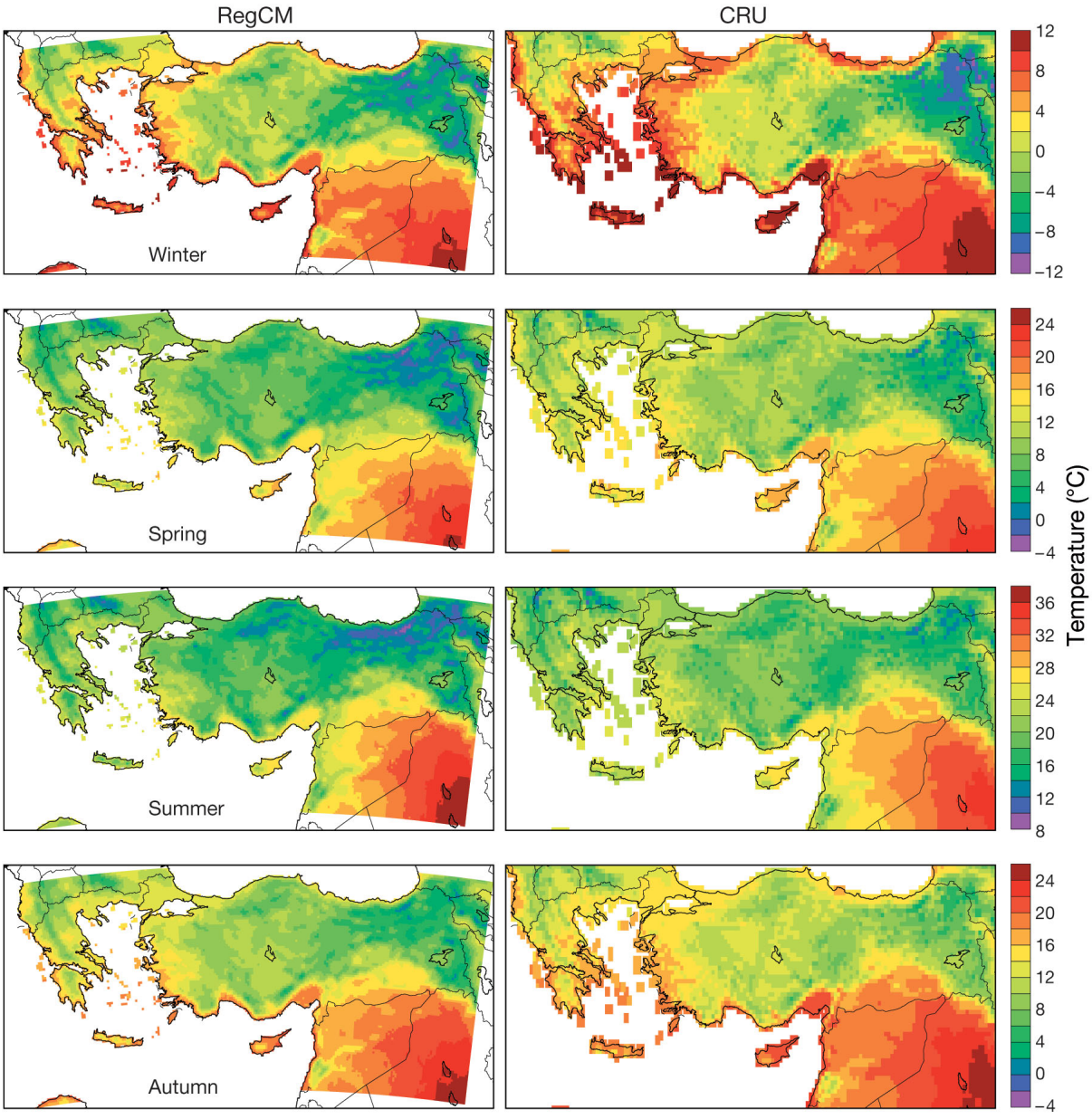

Fig. 4. Comparisons of seasonal mean temperatures (°C) for nested simulations (RegCM, 10 km) and observational data (CRU, 10′), 1961–1990

predictor for the temperature interpolation. Furthermore, the spatial distribution of precipitation in January (1961–1990) for the 10 km simulation over Crete Island is much more consistent with CRU-CL data than with that of the mother domain simulation (Fig. 5, left column). In terms of the 50 km simulation illustrated in Fig. 5, this island is represented by only 3 grid-boxes, which is ineffectual for determining the climatology of any surface variables. In addition, 10 km simulation results agreed with estimated rainfall based on observations over Crete from a previous study (Naoum & Tsanis 2003). They used a rain-gauge network to calculate the estimated rainfall by applying different interpolation schemes.

Precipitation simulations for the summer and autumn seasons agreed well with the CRU-CL data in terms of reproduction of the general pattern and magnitude of precipitation. Especially, the north–south distribution of summer precipitation, which is the dry season in the EM region, is simulated accurately by the regional climate model (Fig. 6). Despite the advantages of gridded observations versus model simulation comparisons, gridded observational data may contain some errors induced by the interpolation

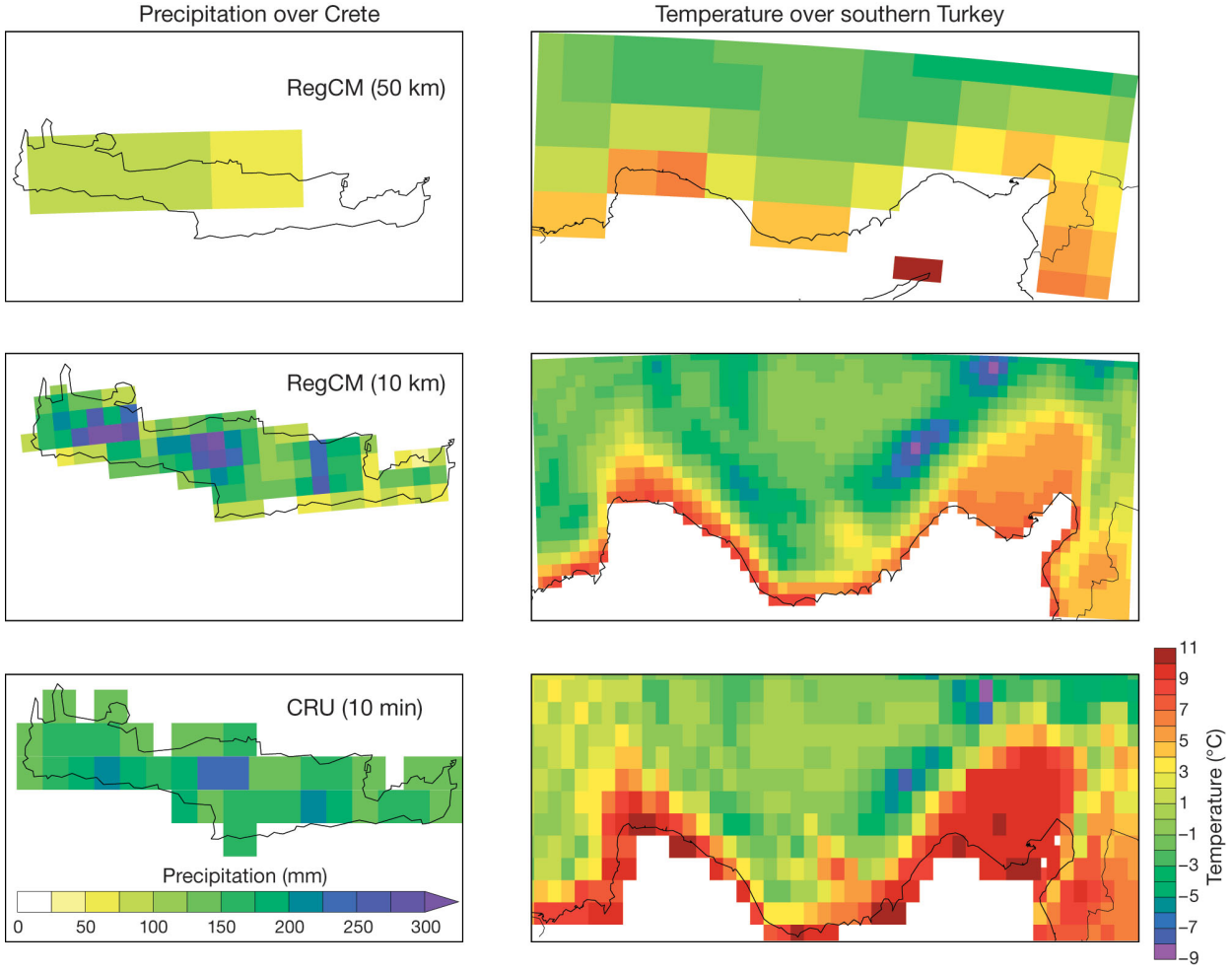

Fig. 5. Comparisons of high-resolution (10′) gridded observations (CRU), and 10 and 50 km simulations (RegCM) for January precipitation over Crete and temperature over southern Turkey (1961–1990)

method for mountainous and coastal regions. Therefore, meteorological station data versus corresponding grid-point comparison is used in the next section for further model validation.

3.3. Coastal stations versus RegCM3 simulations

Since one of the main objectives of the present study was to investigate the added precision of the high-resolution regional climate simulation for coastal regions, all coastal meteorological stations, listed in Table 1, were compared to the RegCM3 simulations. In terms of temperature and precipitation analysis, the stations have been divided into 2 groups covering different time periods (TSMS: 1971–2000; GCN: 1961–1990). The 1971–2000 time period for the stations in Turkey is used because of the better data coverage. Comparison between the stations and simulations was implemented by selecting the closest model grid-point to the station location. A lapse rate correction of 6.5 K km^{-1} was used to correct for elevation difference between the model grid-point and station location, with no other interpolation being performed for temperature. To identify the elevation difference between the 10 and 50 km domain, the results with and without lapse rate correction from both simulations are presented in Fig. 7 (i.e. empty circles represent values with no lapse rate correction).

Grid-point comparisons of simulations with station data indicate that the 10 km temperature simulation bias is lower than that of the 50 km temperature simulation bias for almost all the coastal stations in Turkey (Fig. 7, left). In particular, the temperature bias of the 50 km simulation near the Mediterranean and Black Seas is higher than that of the 10 km simulation; this can be attributed to the fact that a 50 km

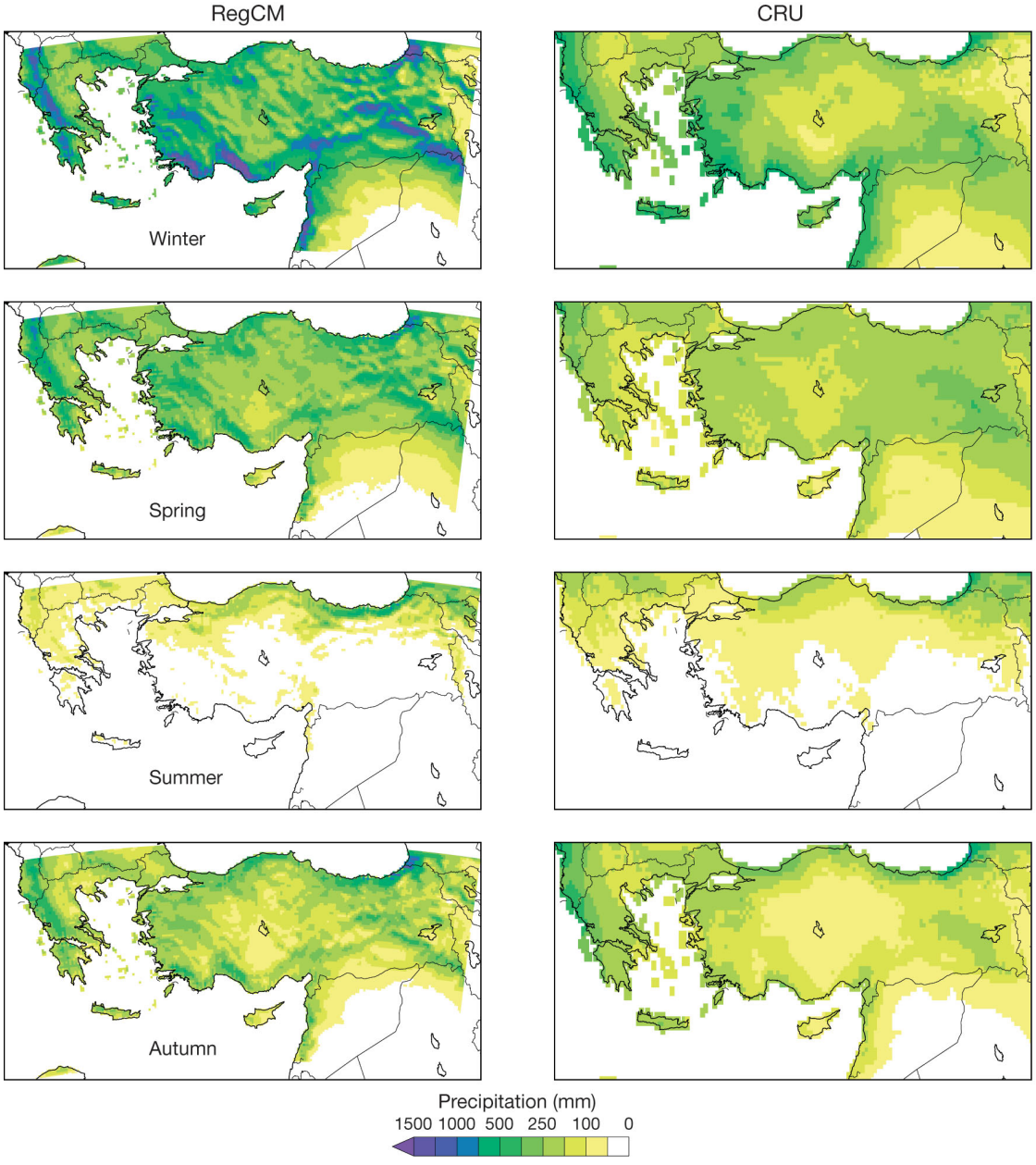

Fig. 6. Comparisons of seasonal mean precipitation for nested simulations (RegCM, 10 km) and observational data (10′)

horizontal resolution is not adequate to resolve the complex terrain in the region. The mean biases of the 10 and 50 km simulations for the stations in the Black Sea region are 0.7° and 1.0°C, respectively. The mean biases for the station in the Mediterranean region are 0.6° and 1.1°C, respectively. The biases over the lowland regions are also the same for the rest of the station locations, 1.1°C.

Comparisons between the GCN stations and model grid-points (Fig. 7, right) are more complicated than the comparisons with TSMS stations because the 12 stations are located over islands, some of which are very small. These stations over small islands tend to be overwhelmed by the influence of sea-surface temperature and large-scale circulation. Therefore, local climate effects related to topography are suppressed in the high-resolution simulation. In the 50 km simulation, only the islands of Crete and Cyprus are represented as a land-surface in the model. The mean biases of the mother and nested domain simulations for the island stations are nearly the same, 1.4°C. The mean biases of the simulations based on the land stations are 1.4° and 1.9°C, respectively. These temperature biases are comparable to previ-

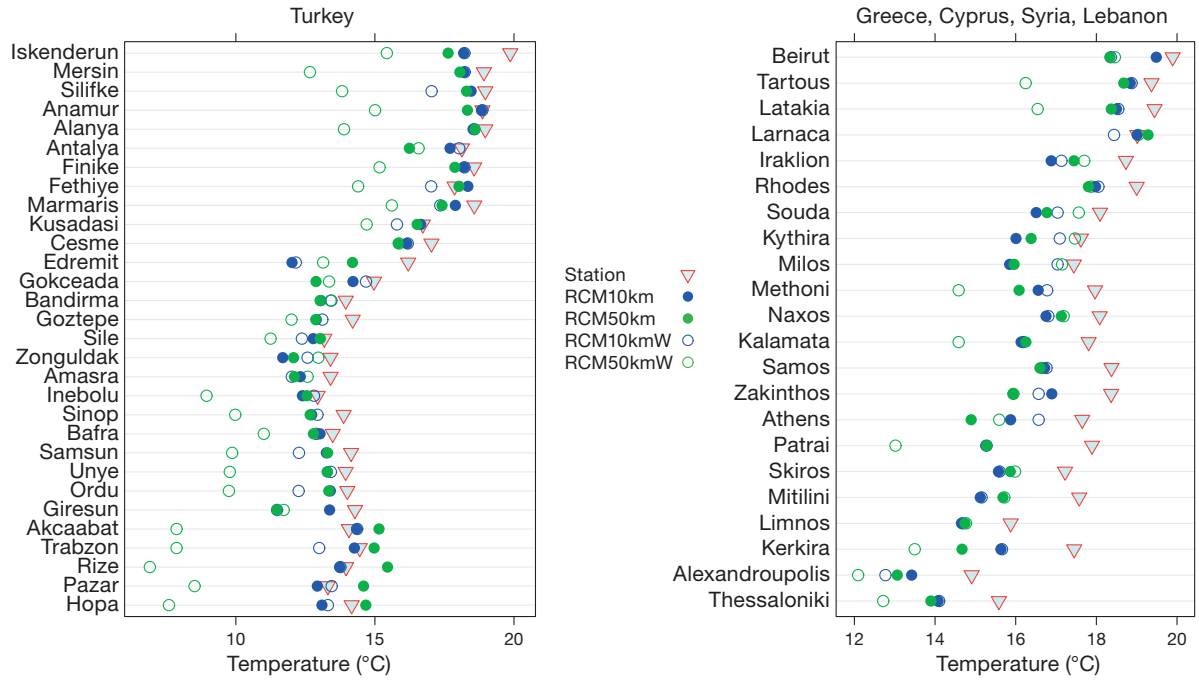

Fig. 7. TSMS (1971–2000, left panel) and GCN (1961–1990, right panel) stations versus corresponding grid-points of regional climate model (RCM) simulations (50 and 10 km) for annual mean temperatures. Filled circles indicate that lapse-rate adjustments have been applied to both simulation grid-points; empty circles: direct values of grid-points. Station details see Table 1

ous 50 km regional climate simulations performed by Moberg & Jones (2004) for Europe, comparing station and grid-box values. In their study, maximum annual mean temperature bias (1961–1990) over Greek stations is positive (1° to 3°C) and the corresponding minimum temperature bias is negative (1° to 3°C).

Fig. 8 compares precipitation at the meteorological stations and the model grid-points. The bilinear interpolation method is applied to estimate simulation results for station locations. The interpolation uses the 4 nearest model grid-points surrounding the station and their weighted distance from the station location to estimate precipitation. It is difficult to measure model performance of simulated precipitation using a point-by-point comparison; therefore, the frequency distributions of relative errors of both simulations are calculated based on all stations for model evaluation (Fig. 9). In terms of the frequency of relative errors, the 10 km precipitation simulation is better than the 50 km simulation based on 52 stations. In the 10 km simulation, the precipitation error is <40% for 46 grid-points out of 52; whereas in the 50 km simulation, 13 grid-points have errors >40%. Moreover, mean biases of the 10 and 50 km simulations are 17 and 42% (Black Sea coast) and 12 and 24% (for the large islands of Crete, Rhodes and Cyprus), respectively. The biases of the 2 simulations are similar for the small islands (18%), where the local climate is influenced to a great extent by the Mediterranean Sea.

In addition to station-based validation, a cross-section, in a north–south direction, of selected model grid-points is given for elevation (m) and precipitation (mm yr^{-1}) (Figs. 10 & 11) to demonstrate the effect of the steep topography on precipitation over coastal regions near the cities of Rize, Trabzon, Giresun and Sinop (Black Sea region) and Antalya, Alanya, Anamur and Silifke (Mediterranean region). In a north–south direction, 10 grid-points from the 10 km simulations were chosen for each of these 8 locations along the coasts of the eastern Black Sea (Fig. 10) and eastern Mediterranean Sea (Fig. 11). The precipitation gradient follows model topography for all locations. Precipitation is reduced on the leeward side of the mountains for all Black Sea locations. The model grid-points rise in elevation to 2000 m within a distance of just 50 km inland, which corresponds to 5 grid-points in the 10 km simulation, from the coastal stations such as Rize, Trabzon and Giresun. This important leeward-side mountain effect along with the sharp gradient in topography are not resolved using the coarser 50 km simulation (not shown). Therefore, the precipitation bias according to the 50 km simulation using just 4 grid-points over the eastern Black Sea coast is 60%, but this is reduced to just 7% using the 10 km simulation.

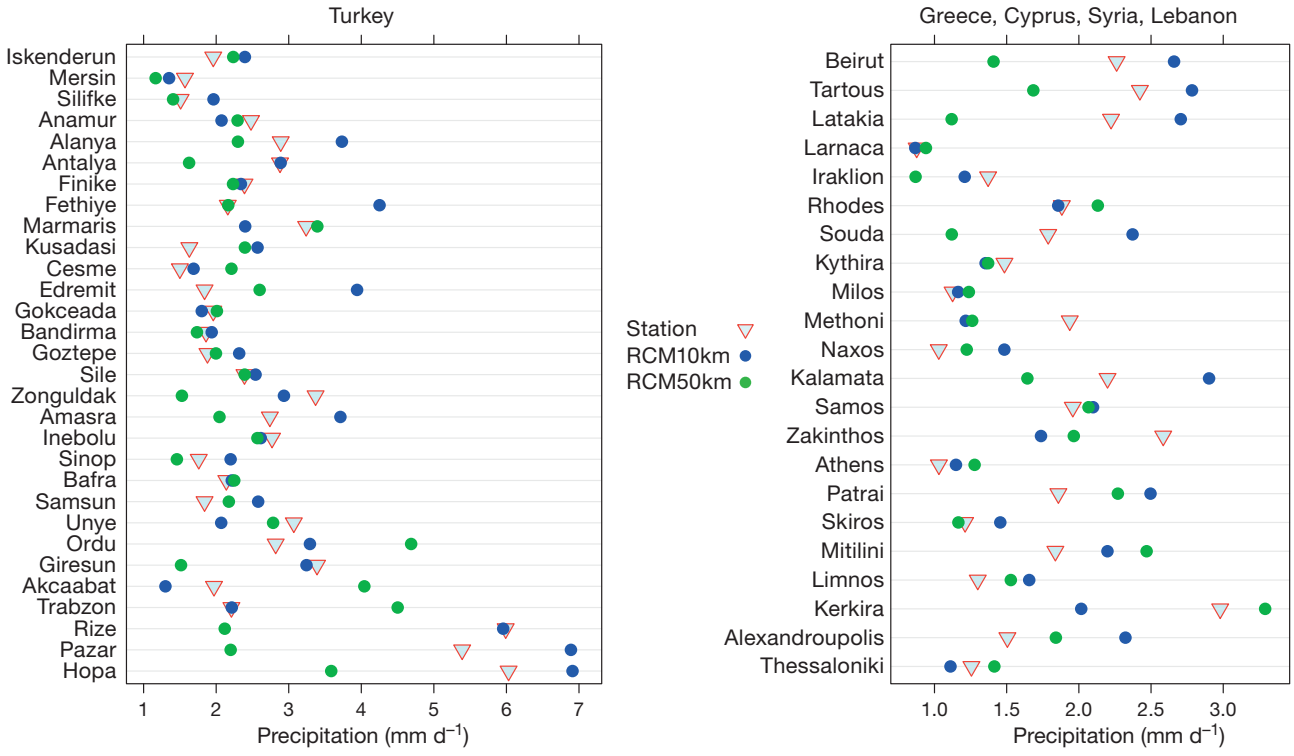

Fig. 8. TSMS (1971–2000, left panel) and GCN (1961–1990, right panel) stations versus corresponding grid-points of regional climate model (RCM) simulations (50 and 10 km) for annual mean precipitation

The precipitation according to the model grid-points located over the Mediterranean coast exceeds 1500 mm within a range of 30 km (3 grid-points in the 10 km simulation) from the sea inland for Alanya and Anamur (Fig. 11). Altitude in the model increases from sea-level to 1000 m within the same horizontal distance for these cities. The precipitation doubles within this distance, helping to reinforce the importance of resolving the model terrain for the local climate along the Mediterranean coast. However, there is only small improvement in the mean bias, from 20% (50 km) to 18% (10 km). Analyzing the distribution of the precipitation simulation and model topography proves that orographic forcing by the eastern Black Sea and Taurus mountains is a significant factor influencing the formation of precipitation along the coast.

3.4. Variability and trends

Station and spatial based analyses for investigating variability and trends are necessary to increase our understanding of high-resolution simulation performance. In terms of defining decadal variability, the 8 stations from TSMS dataset used in the previous section were selected based on the consistency of

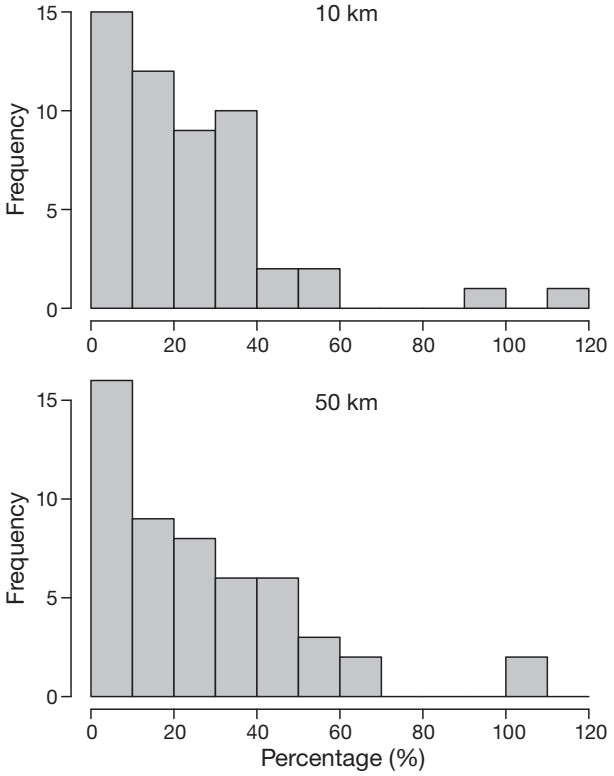

Fig. 9. Precipitation as the percentage error of grid-points for 10 (upper panel) and 50 km (lower panel) simulations based on all 52 stations

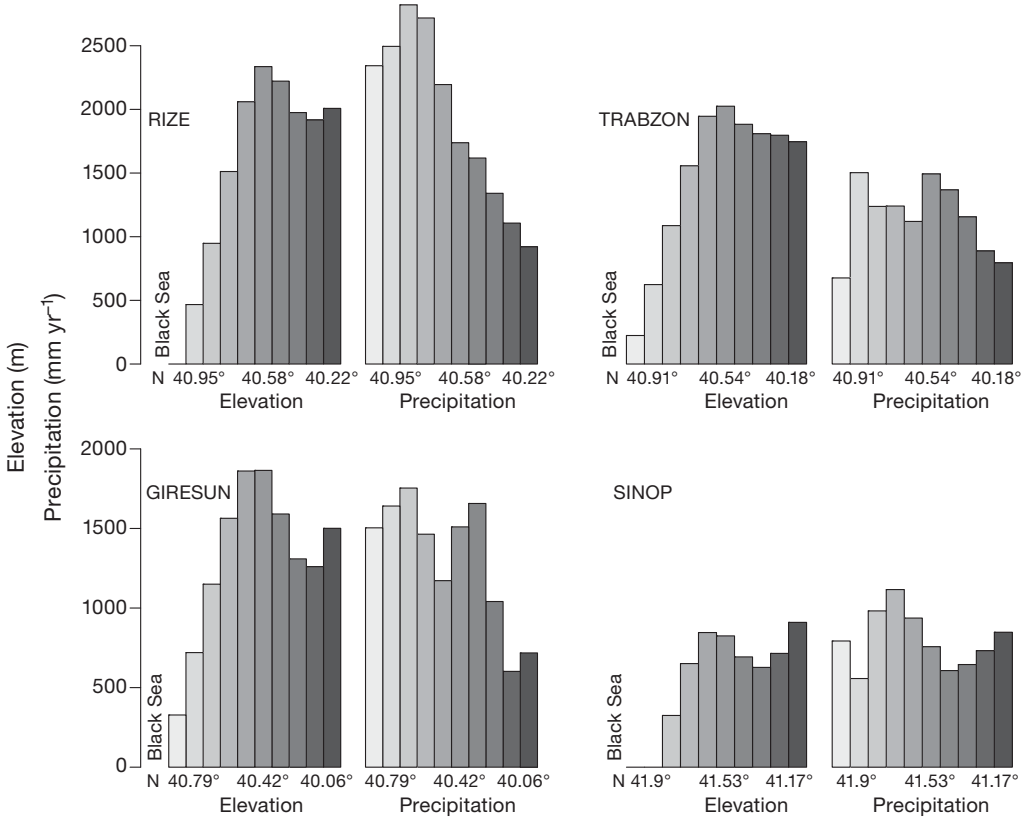

Fig. 10. A cross-section of 10 model grid-points in a north–south direction representing elevation (topography) and annual mean precipitation according to the 10 km simulation. Precipitation induced by topographical gradients between coastal and inland areas is shown for 4 different locations in the Black Sea region

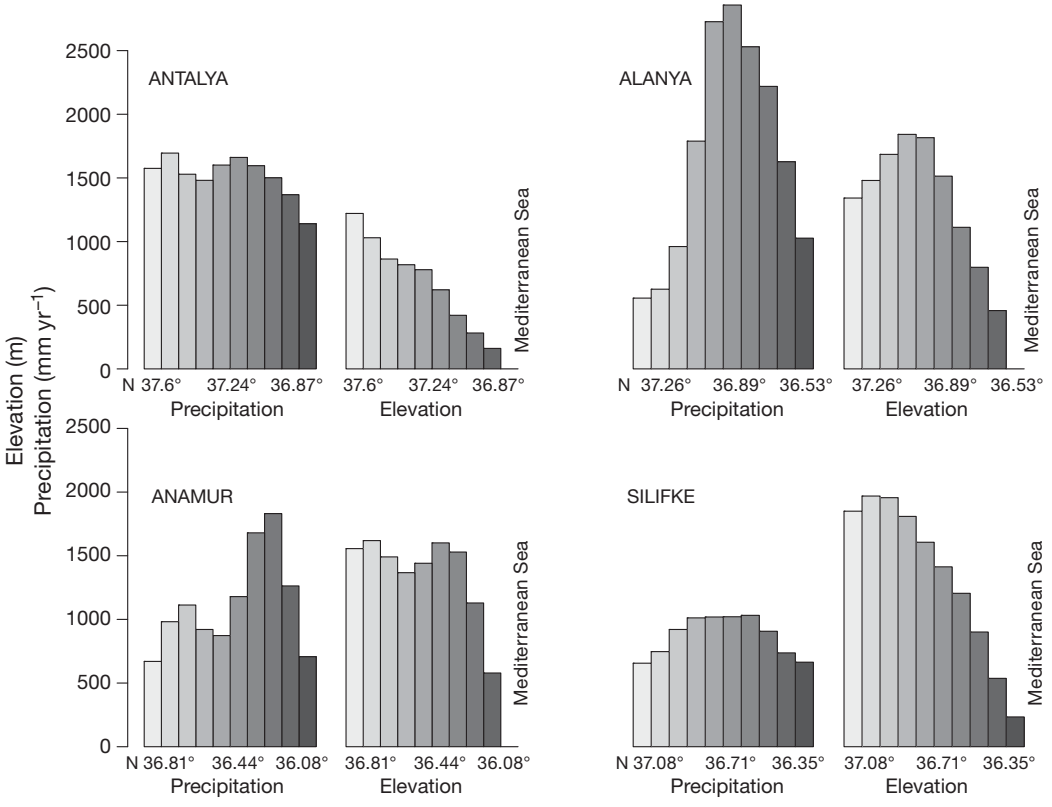

Fig. 11. As in Fig. 10 but for 4 locations near the Mediterranean Sea

analysis. Fig. 12 shows the variability of the Black Sea (left) and Mediterranean region (right) stations (red line) and corresponding grid-points (blue line: 10 km; black line: 50 km) for standardized winter precipitation (1971–2004) calculated using the formula: anomaly of winter precipitation divided by the standard deviation. A 5-point moving average was applied to the model and station data to filter out the interannual variability and help to visualize potential decadal variability or trends. For the Black Sea region, precipitation variability is poorly simulated. Moreover, the statistical correlations are not significant for this region. These results indicate that caution should prevail when applying the model to diagnose precipitation variability or trends for this region. However, the model is capable of capturing the variability for the Mediterranean region. Statistical correlations are notably high for all locations except Antalya, 0.45 for the 10 km simulation. On the other hand, it is important to note that even for this location there is some predictability in the decadal variability as the model captures the positive precipitation trend in both the late 1970s to early 1980s and in the 1990s. The 10 km simulation does not improve the modeled variability over the 50 km simulation when using the station versus grid-box comparison.

Summer temperature over the Mediterranean region has been indicated in previous climate change scenario studies to be the most responsive climate variable (Diffenbaugh et al. 2005, Gao & Giorgi 2008, Önol & Semazzi 2009). Variability for summer temperature in the 10 km simulation is calculated by using decadal anomalies based on the reference period 1961–1990 (Fig. 13). The 10 km simulation illustrates a significant warming trend during the last 5 decades over the EM region (Fig. 13). The warming trend appearing after the first 2 decades of the 21st century is found over the entire EM region. The temperature change in the last decade reaches 2.5°C from central Turkey to the north. This warming trend agrees with gridded observations calculated from the GHCN-CAMS (not shown) and with global surface temperature trends, including the fact that the greatest global anomalies have occurred since 2000 (Hansen et al. 2010).

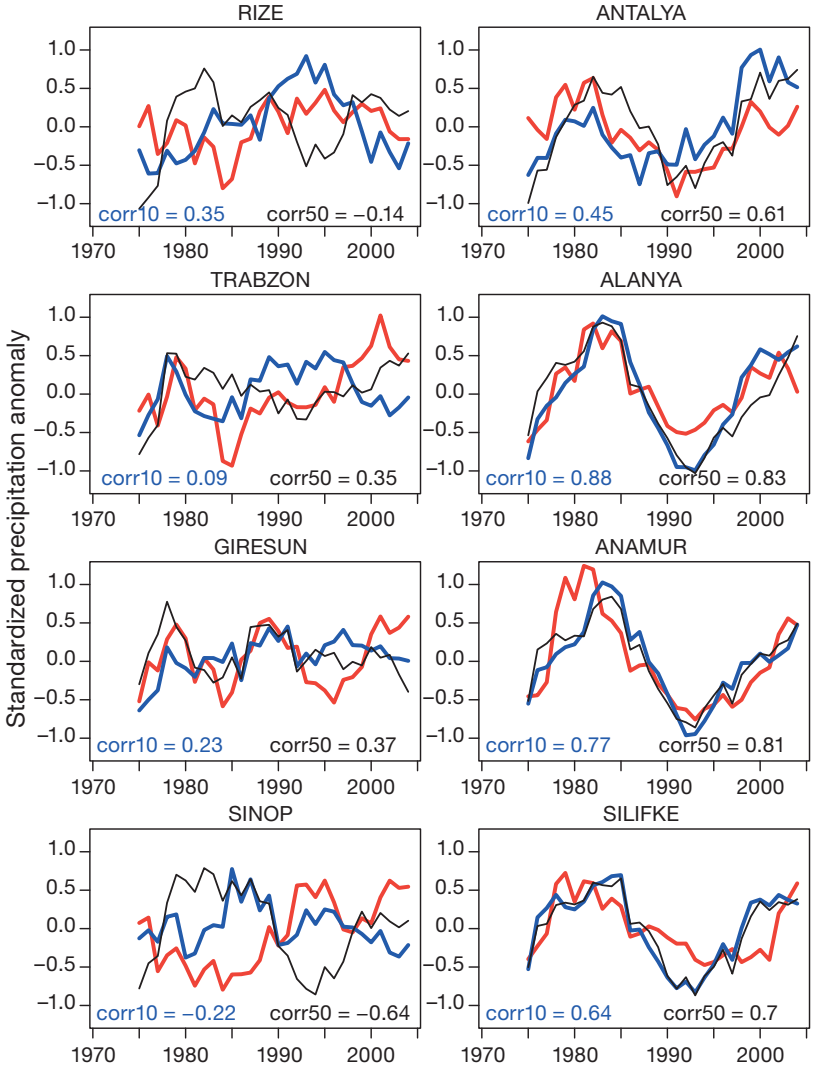

Fig. 12. Variability of observational data (red), nested simulations (blue) and mother simulations (black) for winter precipitation over station locations in the Black Sea (left panels) and Mediterranean Sea (right panels) regions

4. CONCLUSIONS

In this paper, a high-resolution double-nested regional climate simulation driven by NCEP-reanalysis was carried out based on a 48 yr period (1961–2008) in order to examine the impact of horizontal resolution on the simulation of EM coastal regions. Analysis of the 10 km simulation of temperature and precipitation indicates that precision is added by finer resolution of topography. The main conclusions of the present study are given below:

- The 50 km simulated climatology for temperature and precipitation agrees with the several observational datasets.

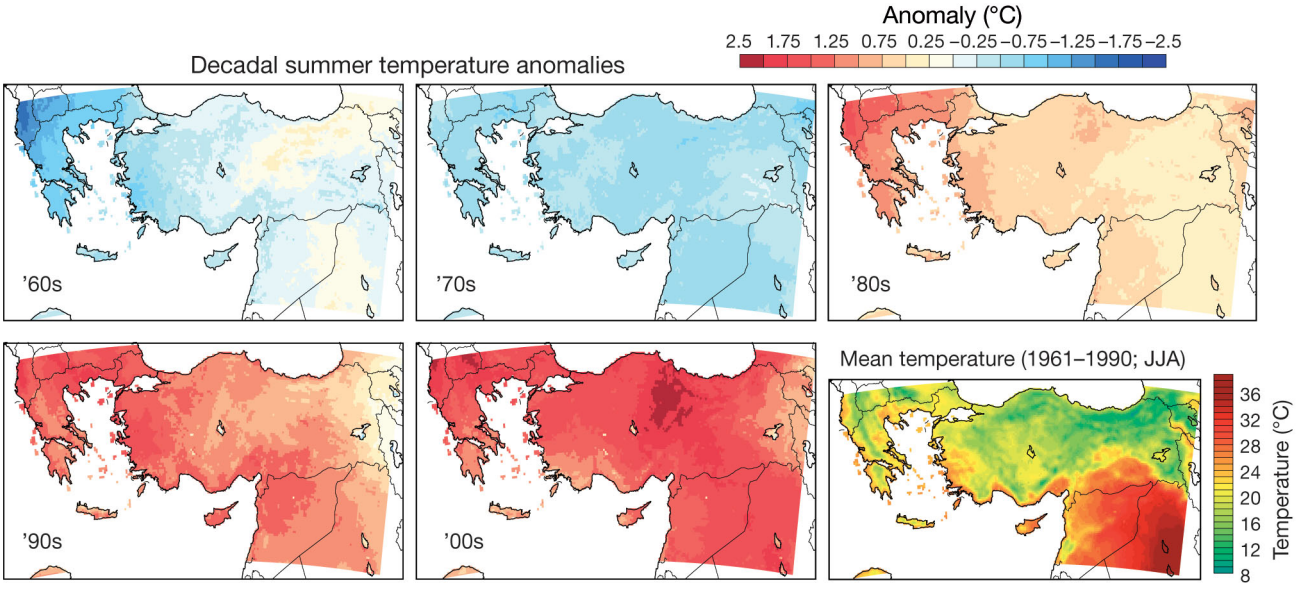

Fig. 13. Decadal anomalies of summer temperature according to nested simulation

- Extreme anomalous events such as the heat wave of July 2007 and winter drought of 1988/1989 are successfully simulated by the 50 km simulation over the EM region.
- In the 10 km nested domain, strong temperature gradients caused by steep topography are well simulated for the eastern Black Sea, the Mediterranean coasts of Turkey and the Ionian coast of Greece when compared to a 10′ observational climatology.
- Analysis of the TSMS station observations and the model grid-points for the 10 and 50 km simulations demonstrated that annual temperature biases are lower in the 10 km simulation for locations where steep mountains are found along the coast.
- Comparing model grid-points to coastal stations also demonstrates that the precipitation error for the Black Sea region, an area with a complex terrain, is smaller (17%) for the 10 km simulation compared to 42% for the 50 km simulation.
- A cross-section analysis comparing elevation in the model to simulated precipitation illustrates the significance of resolving the orographic effects for precipitation.
- Variability of winter precipitation is reproduced by 10 and 50 km model simulations over the Mediterranean region, but variability is poorly simulated for the Black Sea region.
- The significant warming trend of summer temperatures during the last 5 decades is captured over the EM region by the 10 km simulation.

Spatial precipitation comparisons indicate that the difficulty in defining the correct bias for RegCM simulations over mountainous regions is still a major problem due to insufficient observations at high elevations, as has been noted in previous studies. On the other hand, the mean precipitation error of 10 km simulation based on station locations over relatively large islands (Crete, Rhodes and Cyprus) is 12%; this is much lower than the error produced by 50 km simulation, 24%.

Overall, despite the limitations in the horizontal resolution of the hydrostatic model, 10 km simulation results are very promising and indicate that the RegCM3 could be used at this scale over regions with complex terrain to provide more precise climate information. This information over complex terrain could be beneficial in future climate change studies and adaptation strategies, in particular concerning water demands.

Acknowledgements. I acknowledge the National Center for High Performance Computing at Istanbul Technical University for providing the computational platform used to perform the model simulations. I also express my special gratitude to Dr. Jared Bowden for his contribution by proofreading the manuscript.

LITERATURE CITED

Bozkurt D, Sen OL (2011) Precipitation in the Anatolian Peninsula: sensitivity to increased SSTs in the surrounding seas. Clim Dyn 36:711–726

Bozkurt D, Turuncoglu U, Sen OL, Onol B, Dalfes HN (2011) Downscaled simulations of the ECHAM5, CCSM3 and HadCM3 global models for the eastern Mediterranean–Black Sea region: evaluation of the reference period. Clim Dyn doi:10.1007/s00382-011-1187-x

Christensen OB, Christensen JH, Machenhauer B, Botzet M (1998) Very high-resolution regional climate simula-

tions over Scandinavia—Present climate. J Clim 11: 3204–3229

Di Luca A, Elía R, Laprise R (2011) Potential for added value in precipitation simulated by high-resolution nested regional climate models and observations. Clim Dyn doi: 10.1007/s00382-011-1068-3

Dickinson RE, Henderson-Sellers A, Kennedy PJ (1993) Biosphere–Atmosphere transfer scheme (BATS) Version 1E as coupled to the NCAR community climate model. Tech. Rep. TN-387+STR, NCAR, Boulder, CO

Diffenbaugh NS, Pal JS, Trapp RJ, Giorgi F (2005) Fine-scale processes regulate the response of extreme events to global climate change. Proc Natl Acad Sci USA 102: 15774–15778

Evans JP, Smith JP, Oglesby RJ (2004) Middle East climate simulation and dominant precipitation processes. Int J Climatol 24:1671–1694

Fan Y, van den Dool H (2008) A global monthly land surface air temperature analysis for 1948–present. J Geophys Res 113:D01103 doi:10.1029/2007JD008470

Fritsch JM, Chappell CF (1980) Numerical prediction of convectively driven mesoscale pressure systems. I. Convective parameterization. J Atmos Sci 37:1722–1733

Gao XJ, Giorgi F (2008) Increased aridity in the Mediterranean region under greenhouse gas forcing estimated from high resolution regional climate model projections. Global Planet Change 62:195–209

Giorgi F (2006) Climate change hot-spots. Geophys Res Lett 33:L087707 doi:10.1029/2006/GL025734

Giorgi F, Hewitson B, Christensen J, Hulme M and others (2001) Regional climate information—evaluation and projections. In: Climate change 2001: the scientific basis. Contribution of Working Group I to the 3rd Assessment Report of the Intergovernmental Panel on Climate Change. Cambridge University Press, Cambridge, p 583–638

Giorgi F, Jones C, Asrar GR (2009) Addressing climate information needs at the regional level: the CORDEX framework. WMO Bull 58:175–183

Grell GA (1993) Prognostic evaluation of assumptions used by cumulus parameterizations. Mon Weather Rev 121: 764–787

Hansen J, Ruedy R, Sato M, Lo K (2010) Global surface temperature change. Rev Geophys 48:RG4004 doi:10.1029/2010RG000345

Hurrell JW (1995) Decadal trends in the North Atlantic Oscillation: regional temperatures and precipitation. Science 269:676–679

Im ES, Coppola E, Giorgi F, Bi X (2010) Validation of a high-resolution regional climate model for the alpine region and effects of a subgrid-scale topography and land use representation. J Clim 23:1854–1873

Kalnay E, Kanamitsu M, Kistler R, Collins W and others (1996) The NMC/NCAR 40-Year reanalysis project. Bull Am Meteorol Soc 77:437–471

Kanamitsu M, Kanamaru H (2007) Fifty-seven-year California reanalysis downscaling at 10 km (CaRD10). I. System detail and validation with observations. J Clim 20: 5553–5571

Kiehl JT, Hack JJ, Bonan GB, Boville BA, Briegleb BP, Williamson DL, Rasch PJ (1996) Description of the NCAR community climate model (CCM3). NCAR Tech Note, NCAR/TN-420 STR, 152, NCAR, Boulder, CO

Krichak SO, Alpert P, Bassat K, Kunin P (2007) The surface climatology of the eastern Mediterranean region obtained in a three-member ensemble climate change simulation experiment. Adv Geosci 12:67–80

Kuglitsch FG, Toreti A, Xoplaki E, Della Marta PM, Zerefos CS, Türke M, Luterbacher J (2010) Heat wave changes in the eastern Mediterranean since 1960. Geophys Res Lett 37:L04802 doi:10.1029/2009GL041841

Mitchell TD, Jones PD (2005) An improved method of constructing a database of monthly climate observations and associated high-resolution grids. Int J Climatol 25: 693–712

Moberg A, Jones PD (2004) Regional climate model simulations of daily maximum and minimum near-surface temperatures across Europe compared with observed station data 1961–1990. Clim Dyn 23:695–715

Naoum S, Tsanis IK (2003) Temporal and spatial variation of annual rainfall on the island of Crete, Greece. Hydrol Processes 17:1899–1922

New M, Lister D, Hulme M, Makin I (2002) A high-resolution data set of surface climate over global land areas. Clim Res 21:1–25

Önol B, Semazzi FHM (2009) Regionalization of climate change simulations over the eastern Mediterranean. J Clim 22:1944–1961

Pal JS, Small EE, Eltahir EAB (2000) Simulation of regional scale water and energy budgets: influence of a new moist physics scheme within RegCM. J Geophys Res 105: 29579–29594

Pal JS, Giorgi F, Bi X, Elguindi N and others (2007) Regional climate modeling for the developing world: the ICTP RegCM3 and RegCNET. Bull Am Meteorol Soc 88: 1395–1409

Prömmel K, Geyer BB, Jones JM, Widmann M (2010) Evaluation of the skill and added value of a reanalysis-driven regional simulation for alpine temperature. Int J Climatol 30:760–773

Rudolf B, Hauschild H, Ruth W, Schneider U (1994) Terrestrial precipitation analysis: operational method and required density of point measurements. In: Dubois M, Desalmand M (eds) Global precipitation and climate change. Springer-Verlag, Heidelberg, p 173–186

Sotillo MG, Ratsimandresy AW, Carretero JC, Bentamy A, Valero F, Gonzalez-Rouco F (2005) A high-resolution 44-year atmospheric hindcast for the Mediterranean Basin: contribution to the regional improvement of global reanalysis. Clim Dyn 25:219–236

Torma C, Coppola E, Giorgi F, Bartholy J, Pongrácz R (2011) Validation of a high-resolution version of the regional climate model RegCM3 over the Carpathian Basin. J Hydrometeorol 12:84–100

Willmott CJ, Matsuura K (1995) Smart interpolation of annually averaged air temperature in the United States. J Appl Meteorol 34:2577–2586

Zanis P, Kapsomenakis I, Philandras C, Douvis K and others (2009) Analysis of an ensemble of present-day and future regional climate simulations for Greece. Int J Clim 29: 1614–1633

Zeng X, Zhao M, Dickinson RE (1998) Intercomparison of bulk aerodynamic algorithms for the computation of sea surface fluxes using TOGA COARE and TAO data. J Clim 11:2628–2644

Submitted: March 7, 2011; Accepted: December 13, 2011

Proofs received from author(s): February 17, 2012